FORWARD AND INVERSE MODELLING OF GEOTHERMAL MICROSEISMICITY USING TOUGH2 COUPLED WITH AN EARTHQUAKE SIMULATOR

Julius Marvin Rivera[1,2], David Dempsey[2]

[1] Energy Development Corporation, One Corporate Centre Building, Ortigas Centre, Pasig City, Philippines

[2] Department of Engineering Science, University of Auckland, 70 Symonds Street, Auckland, New Zealand

jriv752@aucklanduni.ac.nz.

Keywords: *microseismicity, reservoir modelling, injection, inverse modeling, TOUGH2*

ABSTRACT

Reservoir modelling is undertaken to represent the physical state of the reservoir in order to estimate its current condition and to predict future responses. Prior to use of the reservoir model for forecasting, it is common to calibrate natural state and production models using temperature and pressure data gathered from downhole surveys. In addition to these data, microseismicity presents a further opportunity to calibrate reservoir parameters, in particular the permeability of active faults that serve as major fluid pathways. Microearthquakes (MEQs) occur in areas where brine produced from the production wells is reinjected. The injection causes fluid pressure to build-up in the area, which decreases the rock yield strength and promotes failure: a small earthquake. These events may occur on active faults that are also major fluid pathways in the field. The location, migration, and number of MEQs provide information about pressure change and the nature of fluid flow through the reservoir. Many fields these days are equipped with instruments to detect and locate MEQs. The objective of this project is to integrate MEQ data into the reservoir model development workflow so as to assist model calibration and reservoir characterization.

In this project, a simple reservoir model is created to represent an area into which fluid is injected. A forward run using the TOUGH2 reservoir simulator is conducted to estimate pressure changes due to injection into a single well for specified reservoir and fault parameters. Pressure change on the fault is used to compute an average seismicity rate as well as individual MEQ locations and times. Sensitivity analysis has been conducted to understand how model parameters affect the amount of seismicity generated, and the manner in which it travels along the fault. The coupling between reservoir pressure evolution and synthetic microseismicity provides the physical link necessary to use field MEQ data for calibration. In particular, we will use the seismicity migration rate to estimate permeability of the reservoir and faults. The synthetic study presented here is a proof-of-concept before application of the approach to an actual geothermal MEQ dataset.

1. INTRODUCTION

Geothermal systems involve complex physical processes of heat and mass transfer, and deformation of the solid rock matrix, all in a highly heterogeneous environment (O'Sullivan and Pruess, 2000). Thus, numerical reservoir modelling is usually undertaken to approximate the physical conditions within the reservoir. Numerical simulation is being carried out to mathematically characterize the flow of heat and fluid in a fractured porous media using 3D structures. This 3D model consists of several blocks and elements with each block representing the rocks and faults of the geothermal reservoir. Once the model is a suitable representation of the reservoir, it can be used in forecasting future responses.

Calibration improves the match between the reservoir model and reality. Reservoir models are calibrated by adjusting the reservoir parameters (such as permeability and porosity) so that the simulation matches temperature and pressure data from the field. Usually, these data are measured by downhole surveys. We propose that microseismicity provides an additional source of information for model calibration. Microearthquakes (MEQs) have been commonly considered as one of the tools for assessing reservoir parameters (Pramono and Colombo, 2005) specifically the permeability of the active faults that serve as the major fluid flow paths.

On an active fault, shear stress builds up over time due to tectonic plate motions. An earthquake is triggered when the shear stress reaches the shear strength of the fault. However, for induced seismicity in a geothermal field, the shear strength decreases as the fluid pressure builds up around a reinjection well. This promotes rock failure and triggers small earthquakes. MEQs mainly occur in reinjection areas where brine produced from the production wells is being reinjected. The location, migration, and number of MEQs are essential in providing information on how pressure changes within the field and how fluid flows through the reservoir. Many fields these days are equipped with instruments to detect and locate MEQs. In New Zealand, microseismic networks are operated at five geothermal fields: Wairakei-Tauhara, Kawerau, Rotokawa, Ngatamariki, and Mokai (Sherburn et al, 2015).

This paper will focus mainly on the integration of MEQ data within the reservoir model development workflow. In particular, these data are used during history matching to estimate permeability parameters. Our study is treats only synthetic examples as these initial steps are proof-of-concept. Application of the approach to an actual geothermal MEQ dataset will occur later.

2. METHODOLOGY

This paper follows a general workflow: (1) development of a simple reservoir model for a generic brine reinjection well, (2) development of an induced seismicity model to generate synthetic earthquake observations and (3) inverse modeling of the earthquake observations to estimate permeability of the original (known) reservoir model (Figure 1).

Our generic reservoir model represents an area into which fluid is injected. A forward model run using TOUGH2 is performed using initial reservoir parameters (permeability, porosity, injection rate), which gives as an output pressure changes at different times and locations on a specified fault. The pressure values are used as input for an earthquake simulator that computes the seismicity rate and synthetic microseismicity: number of events in the fault, location and times of earthquakes.

For calibration, the MEQ data generated from the synthetic model are used in inverse modeling to estimate the (known) reservoir parameters. This process yields a probability distribution of the permeability of the specific fault in the model. We achieve this by running several forward models using TOUGH2 and the EQ simulator to estimate the likelihood of different parameter values given the (synthetic) MEQ data.

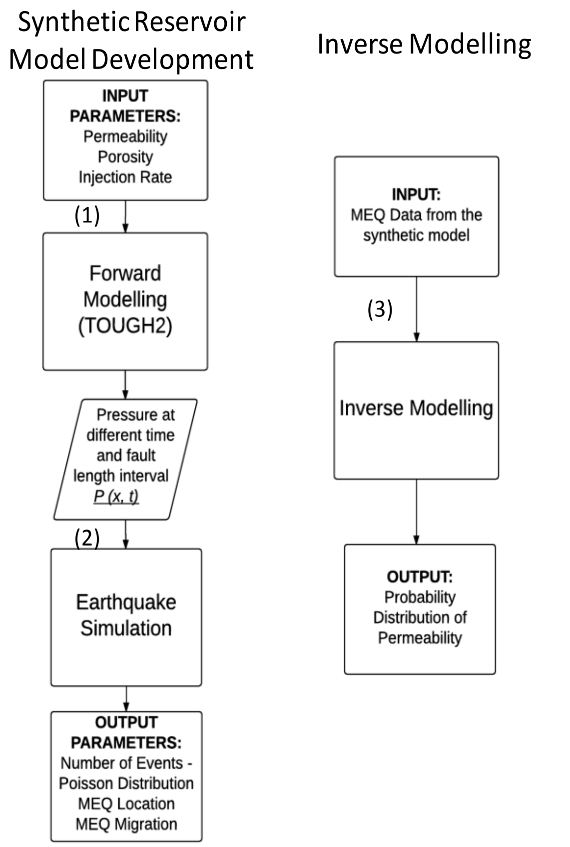

Figure 1: General workflow of the reservoir model development and inverse modeling using microearthquake data.

2.1 Synthetic Reservoir Model Development

2.1.1 Grid Generation

The first step in model creation is generation of grid for flow simulation. For simplicity, a rectangular grid is created to represent the area with fluid being injected at the center. It is important that the dimensions of the blocks are small enough so that running both the forward and inverse models using TOUGH2 will be efficient and accurate. However, for a large grid structure, it will be time-consuming if all blocks are of a small size. PyTOUGH provides mechanisms for controlling and altering grid dimensions, resolution as well as fitting topography and optimizing grid structure (O' Sullivan et al, 2013). Using PyTOUGH, we performed several grid refinements around the model centre where injection occurs (Figure 2a). The original grid, with dimension of 12000 m x 12000 m, consisted of 14,400 blocks with each block having a dimension of 100m x 100m. As we are primarily interested in the area near the injection, the grid generation was modified by increasing the size of the outer blocks to 400m (each side) and performing several refinements to 200m and 100m toward the centre. This reduces the total number of blocks to 5,384.

The model assumes a two-dimensional reservoir with fluid flowing only in x and y directions. The model has only one layer with thickness of 1m. As the fluid is injected at the centre of the grid, it is expected that flow is primarily radial within the reservoir. As a result of the inherent symmetry, flow only needs to be simulated in one quarter of the model grid (Figure 2b). This reduces the grid to 1,346 blocks, which further reduces the time to run simulations. This is important for inverse modeling, in which a large number of forward runs are required.

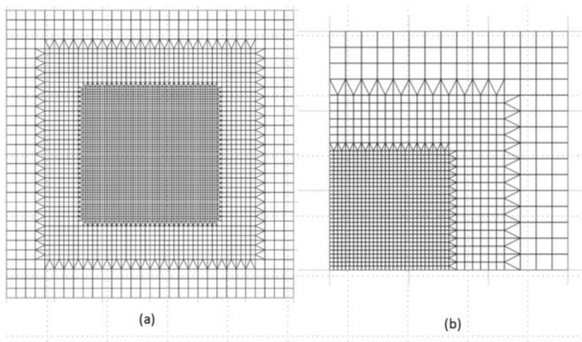

Figure 2: (a) Rectangular grid with increasing refinement at the centre. (b) Quarter of the grid used in the model.

2.1.2 TOUGH2 Data File and Simulation

Prior to running the model, TOUGH2 data files are prepared. In this file, reservoir parameters, generators, and boundary conditions are specified.

For our generic reinjection model, the permeability of the blocks in all directions (x and y) is set to 1.0 x 10^{-13} m^2 with porosity of 0.2. The volume of the boundary blocks is very large (about 10^8 m^3), which approximates an open boundary condition. A generator is placed at the bottom left corner of the quarter grid with injection rate of 1 kg/s and temperature of 50ºC. Initial conditions are set to pressure of 0.1 MPa and temperature of 50ºC, the same as the injection temperature so that only fluid pressure effects are considered. The model is run to an end time of 5 years. The resulting pressure change within the reservoir and spatiotemporal pressure changes on the fault are shown in Figure 3.

In this model, the fault is assumed to have the same permeability as the reservoir (i.e., all the blocks in the model has uniform permeability) thus the pressure change in the model is uniform within the reservoir. However, in a real geothermal system, the permeability of the fault and the reservoir is different. The difference in permeability makes a fault a conduit of the fluid. This will result in different pressure changes within the fault as compared to the homogeneous reservoir.

As seen in Figure 3a, higher pressure is observed in the area near the injection well and the pressure decreases as you move away from it. Also, it is observed that at a given distance from the injection well the pressure initially increases logarithmically in time due to the 2D nature of the flow (Figure 3b). Pressure begins to stabilize at later time due to the imposed open boundary condition.

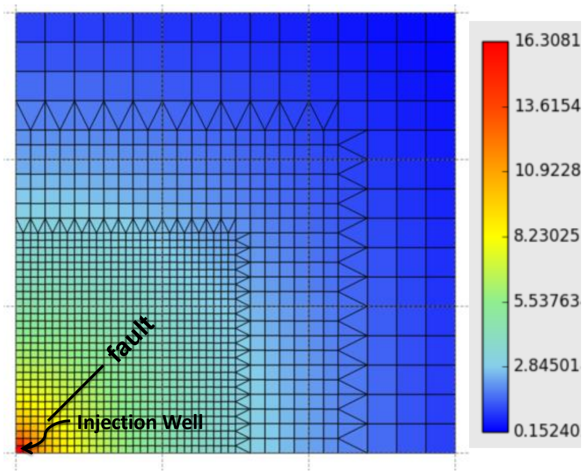

(a)

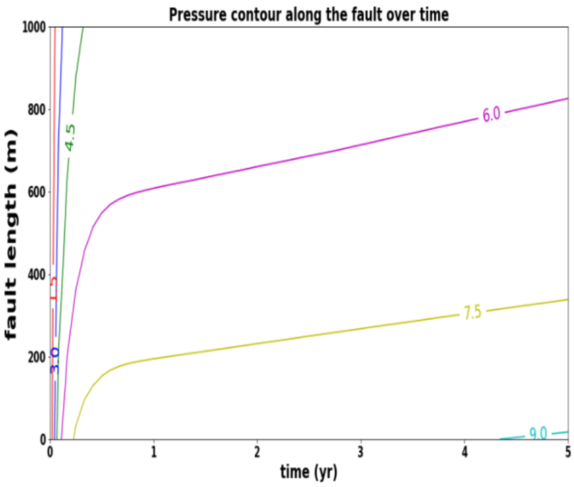

(b)

Figure 3: (a) Pressure change through the fault and the reservoir after 5 yrs. (b) Spatiotemporal pressure change in the fault over time (open boundary).

2.1.3 Induced Seismicity from Pressure Data

The pressure output from the TOUGH2 simulation is used in generating synthetic earthquakes on the active fault. We approximate a fault as a line segment contained within a two-dimensional reservoir (see Figure 3a). Pressure output from the reservoir simulation that is coincident with the position of the imagined fault is used to estimate a spatiotemporal seismicity rate. The pressure output is interpolated depending on the location of the fault in the reservoir model (e.g., length of fault, distance from injection, etc). The details of the fault in this study are given in Table 1.

Fault Parameters	
Fault Length (L)	1000m
Fault Azimuth	45 °
Distance from the Injection	500m
Angle of Fault from Injection	45 °

Table 1: Fault parameters in generating seismicity rate

The seismicity rate of the reservoir is estimated based on the pressure evolution in the active fault which affects the shear strength of the formation. The relationship of shear stress and strength provides information on seismicity. For induced seismicity, the shear strength changes depending on the fluid pressure in the fault. Shear strength (τ_s) is given by the equation:

$$\tau_s = f_s(\sigma_n - p)$$

Where f_s is the friction coefficient, σ_n is the normal stress, and p is the fluid pressure.

The fault is considered stable and will not trigger earthquakes if the shear strength is larger than the shear stress. However, when there is fluid injection, pressure build-up will decrease the shear strength. If this continues and the shear strength decreases until it equals the shear stress, i.e., $\tau_s = \tau$, then an earthquake will be triggered. The pressure build-up required to trigger the first earthquake is the critical pressure (p_{crit}) of the fault.

To estimate the total seismicity rate, the fault is divided into equal segments (Δx). For each segment in which $\tau < \tau_s$, no seismic event is expected. If $\tau = \tau_s$, the fault is expected to reach failure and thus a seismic event occurs. There is no case in which $\tau > \tau_s$. Given, this, the average number of events (N) generated in the fault at a given length (L) and at a given time (t) is (Dempsey and Suckale, 2017):

$$N = k\int_0^L \int_0^t [\Delta\tau(x,t) - \Delta\tau_s(x,t)\ \delta(\tau(x,t) - \tau_s(x,t))\, dx\, dt$$

The k in the equation is a proportionality constant that accounts for other relationships between the stress and microseismicity. This constant can also be used as a parameter to scale the integrated seismicity rate to choose the total number of earthquakes that are modelled. The second part of the equation $[\delta(x)]$ is the Dirac delta function, which has the following properties:

$$\delta(x) = \begin{cases} 0, & x \neq 0 \\ \infty, & x = 0 \end{cases} \quad \text{and} \quad \int_{-\infty}^{\infty} \delta(x)\, dx = 1$$

Given the pressure data of the fault based on the fault details stated above, the number of events is then calculated. For our study, we assign the critical pressure, $p_{crit} = 0$, and the number of segments (Δx) to 200. The seismicity rate is simulated for the 5 year duration of the reservoir simulation (Figure 4).

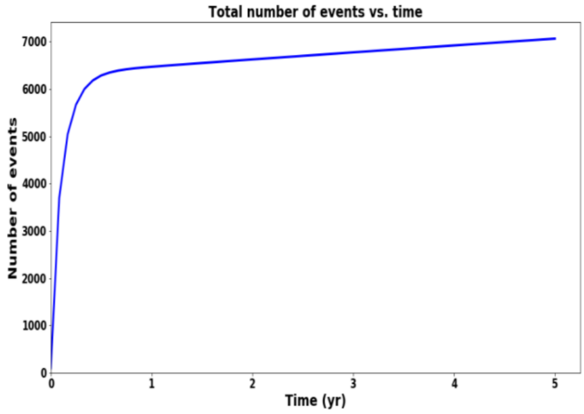

(a)

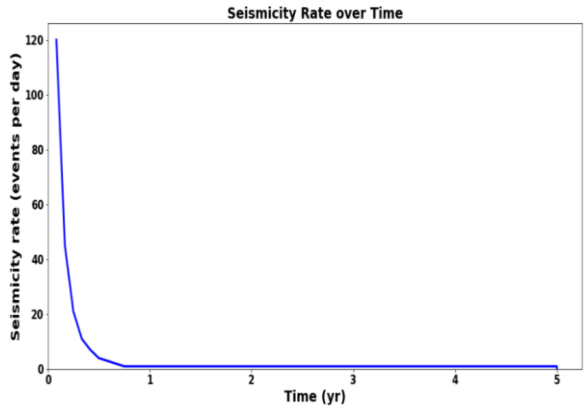

(b)

Figure 4: (a) Average total seismicity generated on the fault over time. (b) Seismicity rate (number of events per day) over time

2.1.4 Generation of MEQ Data

Earthquake occurrence contains an element of randomness: the magnitude, location, and the time cannot be predicted ahead of time. The uncertainty of earthquake triggering can be described by a Poisson point process given that:

1. The occurrence of earthquake is random within a given time period, and
2. The events are independent of each other.

The seismicity rate gives an idea of how many seismic events may occur in a given time interval. However, due to its random nature, the number of events in a time interval may not be exactly the same as that seismicity rate integrated over that interval. For example, the seismicity rate in a particular area might be 10 events per year *on average*, however, the actual recorded number of events could be 9 in one year, 11 the next, and 12 the year after.

In this paper, the discrete Poisson distribution is used to generate random events within a given time interval. The synthetic earthquake data we generate is random so that each time we rerun the simulation, different earthquakes are obtained (Figure 5). The dataset may be completely different but both sets still represent the same seismicity rate. The first dataset presented in Figure 5 has about 3000 MEQs and we use this as the synthetic MEQ data for inverse modelling.

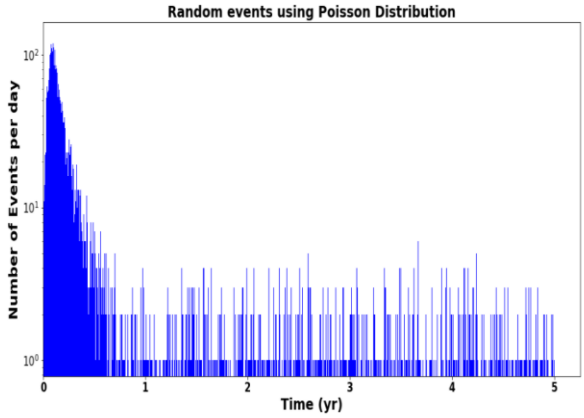

(a)

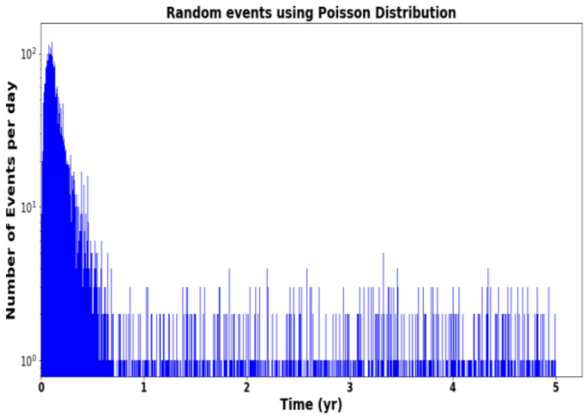

(b)

Figure 5: Seismic datasets generated using Poisson distribution (two different dataset of same seismicity rate)

2.2 Inverse Modelling

Calibration using the MEQ data is done by adjusting reservoir parameters in order to match approximately the occurrence times of earthquakes. To achieve this, we run several forward models of the TOUGH2 reservoir simulation, convert the pressure output to a seismicity rate, and then compare this to the synthetic MEQ data. Due to uncertainty in the earthquake observations, the reservoir parameters cannot be established uniquely. They are instead represented as a probability distribution. From basic knowledge of the permeability of geothermal systems, the lower and upper bounds of permeability are assumed. For natural geothermal systems, the value of the bulk permeability typically lies between the range of 10^{-14} to 10^{-13} m^2 (Wallis, 2015). We guess permeability values in this range and then run a forward simulation for each to generate different seismicity rates (after Fig. 4). For this study, we considered 100 forward model runs of different permeability values ranging from 5.0×10^{-14} to 5.0×10^{-13} m^2.

These seismicity rate models are then scored using the log likelihood distribution for a non-homogeneous Poisson process given by Lindqvist and Taralsden (2013):

$$LLK = \sum_{i=1}^{n} \ln(\lambda(t_i,\theta)) - \int_{0}^{t_n} \lambda(u,\theta)du$$

In this equation, θ is the parameter value we are seeking to constrain in the seismicity rate model, which in the case of our study is the permeability of the fault. The MEQ data is compared to the seismicity rates generated from the range of permeability values, then all LLK values are plotted to generate a likelihood distribution. This summarizes the estimated permeability of the reservoir in a probabilistic sense. For the MEQ data generated from the synthetic model, the likelihood distribution is shown in Figure 6. As seen in the plot, the permeability of $1x10^{-13}$ used in the synthetic reservoir model occurs within the range of most likely estimate value which gives us the higher confidence of obtaining a well-calibrated model.

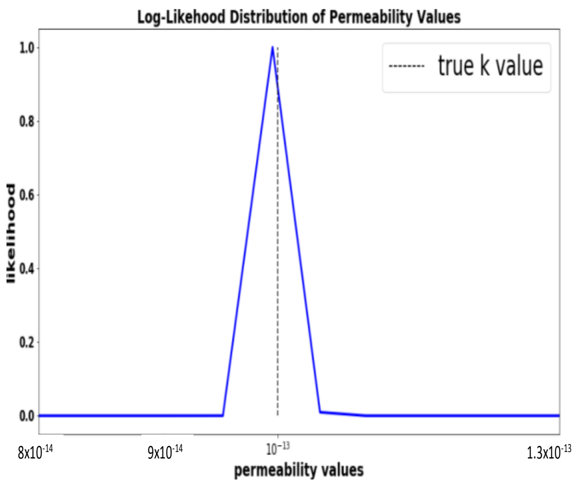

Figure 6: Likelihood distribution of 100 forward model runs to estimate permeability of the reservoir using the 6832 synthetic MEQ data. The black dashed line shows the true value used to generate the synthetic data.

The likelihood distribution shown above is computed based on 6832 MEQs simulated from the synthetic model. While it is quite narrow and centred on the true permeability value, this changes depending on the number of MEQ data available for calibration. For example, a dataset with fewer MEQs (say, from a shorter period of time) will be wider, reflecting greater uncertainty when less data are available for calibration (Figure 7a). We have considered three examples, for earthquake data gathered over 1, 2 and 5 years with 6247, 6392, and 6832 events, respectively. It is clear that greater confidence in the estimated permeability is achieved for longer periods of seismic monitoring, because the likelihood distributions are narrower and peaked closer to the true permeability value.

A similar response of the likelihood distribution is observed when there is less MEQ data gathered within a fixed span of time (Figure 7b). This corresponds to the situation of seismic networks of varying sensitivity. As an example, a dataset with MEQ recorded 6832 events in 5 years gives a higher confidence (less uncertainty) as compared to datasets of 70 or 700 events. Worse still, there is a degree of arbitrariness due to the random nature of the events. For example, a different set of 70 events, drawn from the same underlying earthquake distribution, yields a quite different likelihood distribution.

3. CONCLUSION

This paper presents a theoretical method for the use of microearthquake data in the calibration of reservoir models, specifically in the estimation of permeability. The occurrence of miroearthquakes depends on simulated pressure build-up on a fault due to nearby injection. As pressure increases, yield strength decreases, which promotes rock failure and triggers seismic events. Whether simulated pressure increase in the fault is sufficient to trigger an earthquake is based on the critical pressure of the reservoir. We use these ideas to first simulate the average number of events along a fault (the seismicity rate), and then use this information to generate random earthquakes (synthetic data).

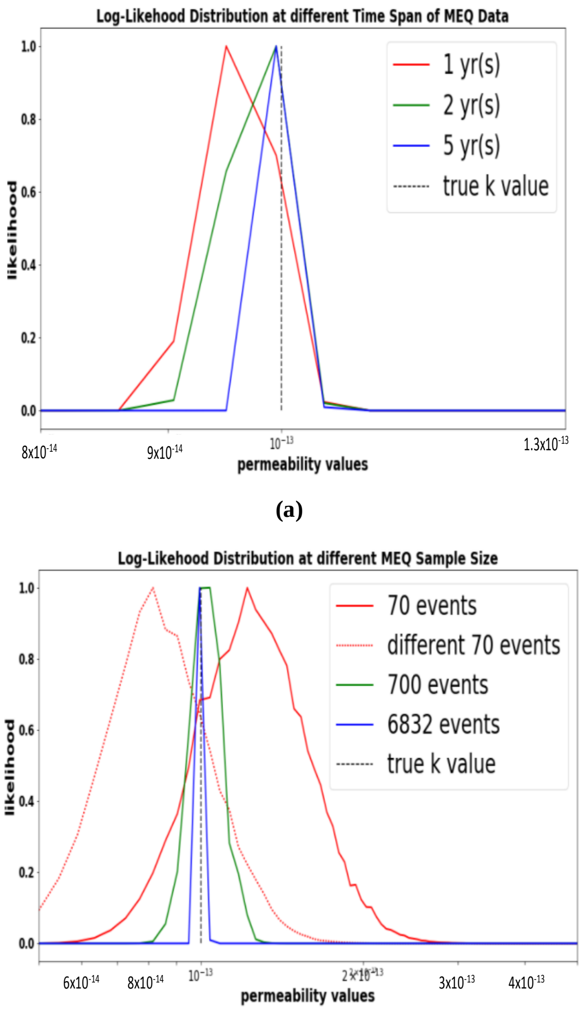

Figure 7: Likelihood distributions for different synthetic MEQ datasets: (a) a shorter observation period, and (b) a less sensitive network (bottom).

Calibration of a reservoir model using MEQ data is based on a likelihood approach. Given some earthquake measurements, the method outputs a probability distribution for reservoir permeability, which has a strong control on pressure build-up and hence seismicity. Our approach to inverse modeling was to generate several forward runs with different permeability values and to compare the simulated seismicity for each against a set of synthetic MEQ observations (using the log likelihood distribution for a nonhomogeneous Poisson process). Our results suggest that it is possible to identify reservoir parameters, providing there are a sufficient number of events recorded. However, this requires that we know with high confidence other parameters on which the model relies. When there is less MEQ data, the probability distribution for permeability is wider and the uncertainty is greater.

The next step in this study is adapting our approach to estimate multiple reservoir parameters, e.g., reservoir and fault permeability separately. We would then look to apply the approach to a real set of measured MEQ data.

ACKNOWLEDGEMENTS

We would like to thank The University of Auckland for the opportunity to develop and execute this study. Also, we would like to express our gratitude to Energy Development Corporation and New Zealand ASEAN Scholarship for their support in pursuing this project and the thesis study.

REFERENCES

Croucher, A. E. *PyTOUGH User's Guide*, University of Auckland, Auckland, New Zealand, github.com/acroucher/PyTOUGH (2000).

Croucher, A. E. *PyTOUGH: a Python scripting library for automating TOUGH2 simulations*. Proceedings (electronic) 33rd New Zealand Geothermal Workshop (2011).

Dempsey, D. E. and Suckale, J. *Physics-based forecasting of induced seismicity at Groningen gas field, the Netherlands*. Geophysical Research Letters 44, doi: 10.1002/2017GL073878 (2017).

Greenhough, J. and Main, I.G., *A Poisson model for earthquake frequency uncertainties is seismic hazard analysis*. Geophysical Research Letters 35, doi: 10.1029/2008GL035353 (2008).

Lindqvist, B.H. and Taraldsen, G. *Exact statistical inference for some parametric nonhomogeneous Poisson processes*. J. Iranian Stat. (2013).

O'Sullivan, M. J. and Pruess, K. *Geothermal Reservoir Simulation: The State-of-Practice and Emerging Trends*. World Geothermal Congress (2000).

O' Sullivan J., Dempsey D., Croucher A. et. al. *Controlling Complex Geothermal Simulations using PYTOUGH*. 38th Workshops on Geothermal Reservoir Engineering (2013).

Pramono, B. and Colombo, D. *Microearthquake Characteristics in Darajat Geothermal Field, Indonesia.* World Geothermal Congress (2005).

Pruess, K., Oldenburg, K. & Moridis, G. *TOUGH2 user's guide, version 2.0*, Lawrence Berkeley National Laboratory, University of California, Berkeley (1999).

Sewell, S.M., Cumming, W., et. al. *Interpretation of Microearthquakes at the Rotokawa Geothermal Field, 2008 to 2012*. Proceedings of 35th New Zealand Geothermal Workshop (2013).

Sherburn, S., Bromley, C., et. al. *New Zealand Geothermal Induced Seismicity: an overview*. Proceedings World Geothermal Congress (2015).

Wallis, I., Moon, H. et. al., *Perspectives on Geothermal Permeability*. Proceedings of 37th New Zealand Geothermal Workshop (2015).